Biochemical Pharmacology 83 (2012) 671–679

Contents lists available at SciVerse ScienceDirect

Biochemical Pharmacology

journal homepage: www.elsevier.com/locate/biochempharm

Molecular effects of gallium on osteoclastic differentiation of mouse and human monocytes

E. Verron [a,b,d,*], A. Loubat [c], G.F. Carle [a], C. Vignes-Colombeix [d], I. Strazic [d], J. Guicheux [d], N. Rochet [a], J.M. Bouler [d], J.C. Scimeca [a]

[a] GéPITOs, Université de Nice, CNRS, UMR 6235; UFR Médecine, 28 avenue de Valombrose, 06107 NICE, cedex 2, France
[b] GRAFTYS SA, Aix En Provence, France
[c] IFR50, Université de Nice, Service de Cytométrie Pasteur; UFR Médecine, 28 avenue de Valombrose, 06107 NICE, cedex 2, France
[d] INSERM U791, Faculté de Chirurgie Dentaire, Nantes, France

ARTICLE INFO

Article history:
Received 13 October 2011
Accepted 12 December 2011
Available online 19 December 2011

Keywords:
Gallium
Osteoclast
CD11b$^+$
NFATc1
NFκB
Calcium

ABSTRACT

We had previously reported that gallium (Ga) inhibited both the differentiation and resorbing activity of osteoclasts in a dose-dependent manner. To provide new insights into Ga impact on osteoclastogenesis, we investigated here the molecular mechanisms of Ga action on osteoclastic differentiation of monocytes upon Rankl treatment. We first observed that Ga treatment inhibited the expression of Rankl-induced early differentiation marker genes, while the same treatment performed subsequently did not modify the expression of late differentiation marker genes. Focusing on the early stages of osteoclast differentiation, we observed that Ga considerably disturbed both the initial induction as well as the autoamplification step of *Nfatc1* gene. We next demonstrated that Ga strongly up-regulated the expression of *Traf6*, *p62* and *Cyld* genes, and we observed concomitantly an inhibition of IκB degradation and a blockade of NFκB nuclear translocation, which regulates the initial induction of *Nfatc1* gene expression. In addition, Ga inhibited *c-Fos* gene expression, and subsequently the auto-amplification stage of *Nfatc1* gene expression. Lastly, considering calcium signaling, we observed upon Ga treatment an inhibition of calcium-induced Creb phosphorylation, as well as a blockade of gadolinium-induced calcium entry through TRPV-5 calcium channels. We identify for the first time Traf6, p62, Cyld, IκB, NFκB, c-Fos, and the calcium-induced Creb phosphorylation as molecular targets of Ga, this tremendously impacting the expression of the master transcription factor Nfatc1. In addition, our results strongly suggest that the TRPV-5 calcium channel, which is located within the plasma membrane, is a target of Ga action on human osteoclast progenitor cells.

1. Introduction

Gallium (Ga) was discovered in 1875 by the French chemist Paul-Emile Lecoq de Boisbaudran, who choose this name in honor of Gallia (France) [1]. In the early 1970s, it was demonstrated that Ga had several therapeutic uses including (i) the decrease of accelerated bone mineral resorption, which occurs during osteolytic bone diseases, and the subsequent lowering of elevated plasma calcium levels associated with these pathologies; (ii) the inhibition of neoplastic proliferation; (iii) the treatment of some intracellular pathogens such as species of *Mycobacterium* [2]. Studies on Ga, which were mainly focused on its antitumor activities [3], have shown that Ga caused a mild hypocalcemia [4]. In this context, Ga has been used to treat hypercalcemia resulting from malignant tumors such as parathyroid carcinoma and Paget's disease of bone [5–7]. This antihypercalcemic effect of Ga results from an inhibition of bone resorption rather than an increase of urinary calcium excretion [5,8]. Indeed, due to its chemical characteristics, Ga presents an affinity for biological apatite that explains the presence of Ga deposits in bone tissue, and preferentially at sites of rapid bone remodeling such as active metaphyseal growth plate and healing fractures [9–11].

Despite these observations, few studies have explored the effect of Ga on bone cells [8,12,13]. Hall et al. demonstrated that Ga inhibited bone resorption in a dose-dependent manner, and for example, at 100 μg/mL, Ga reduced the resorption activity by 64% without inducing modifications to the morphology or number of osteoclasts [12]. In contrast to these findings, Blair et al. showed a cytotoxic effect of Ga on osteoclasts [13]. Considering this discrepancy, we previously investigated the biological effect of

* Corresponding author at: INSERM U791, Faculté de Chirurgie Dentaire, 1, place Alexi Ricordeau, 44042 Nantes, France. Tel.: +33 2 40 41 29 16; fax: +33 2 40 08 37 12.
E-mail address: elise.verron@univ-nantes.fr (E. Verron).

0006-2952/$ – see front matter © 2011 Elsevier Inc. All rights reserved.
doi:10.1016/j.bcp.2011.12.015

Ga on bone cells. We reported that Ga inhibited both the differentiation and the resorbing activity of osteoclasts in a dose-dependent manner (0–100 μM) [14]. Furthermore, Ga did not affect the viability or proliferation of osteoblasts. Despite these results strongly suggesting a therapeutic potential of Ga, many unknowns remain concerning the mechanism of Ga action. With this in mind, we examined the molecular mechanisms of Ga action on osteoclasts.

Osteoclasts are giant multinucleated cells of monocyte-macrophage origin that degrade bone matrices [15]. RANKL (receptor activator of NFκB ligand) and M-CSF (macrophage colony stimulating factor) are the critical factors that regulate osteoclastic differentiation [16]. RANKL is expressed by osteoblasts and triggers pre-osteoclast differentiation [17] whereas M-CSF, secreted by osteoblasts, provides differentiated cells with a survival signal [18]. RANKL strongly induces the expression of nuclear factor of activated T cells, cytoplasmic 1 (Nfatc1), a transcription factor that is a master regulator of osteoclast differentiation. Nfatc1 induction is dependent on both NFκB and *c-Fos* pathways [19–22]. More specifically, the initial induction of Nfatc1 synthesis requires the activation of the NFκB pathway through the signaling molecule Traf6 (tumor necrosis factor receptor-associated factor 6), as well as the nuclear translocation of the transcription factor Nfatc2, that is constitutively expressed in precursor cells. Upon RANKL binding to its receptor RANK, the complex cooperates with costimulatory receptors to activate calcium signaling that stimulates both the initial induction and the auto-amplification phase of Nfatc1 expression [23]. Indeed, Nfatc1 binds to its own promoter, thus leading to robust induction of Nfatc1 protein synthesis [20,24]. An activator protein (AP)-1 complex containing RANKL-activated *c-Fos* is also required for the auto-amplification of Nfatc1 [23]. Eventually, AP-1/Nfatc1 complexes turn on a transcriptional program leading to the expression of osteoclast-specific genes, and the acquisition of mature phenotypic markers such as tartrate-resistant acid phosphatase (Acp5), calcitonin receptor (Ctr), matrix metalloproteinase 9 (Mmp9), integrin-β3 (Itg-β3) or a specific osteoclastic proton pump namely ATP6V0A3.

In this study, we investigated Ga effects on RANKL-induced osteoclastic differentiation of monocytes, comparing first the early and late stages of the process. We next focused on molecular events governing osteoclastic differentiation in its early phase, including the regulation of *Nfatc1* gene expression. Lastly, we hypothesized that Ga may act on calcium uptake and we tested this hypothesis.

2. Materials and methods

2.1. Materials

Alpha minimal essential medium (α-MEM), Dulbecco's Modified Eagle's Medium (DMEM), antibiotic mixture (P/S; 100 U/mL penicillin, 100 μg/mL streptomycin), phosphate-buffered saline (PBS), Hanks' Balanced Salt Solution (HBSS), ionomycin, Fluo-3AM and Fura-RedAM were purchased from Invitrogen Corporation (Paisley, UK). Fetal calf serum (FCS), culture plates and plastics were obtained from Dominique Dutscher (Brumath, France). Gallium nitrate and gadolinium nitrate were obtained from Sigma (Saint Quentin Fallavier, France). Recombinant human M-CSF and RANKL were provided by PeproTech (Rocky Hill, NJ, USA).

2.2. Cell culture

RAW 264.7 cell line (Ref. # TIB-71) was obtained from ATCC (LGC Standards, Molsheim, France). Cells were cultured in DMEM containing 5% fetal bovine serum (Hyclone serum, Thermo Fisher Scientific, Brebière, France). For osteoclastic differentiation experiments, RAW 264.7 cells were seeded at 5000 cells/cm^2 in α-MEM containing 5% Hyclone serum and effectors were added immediately. RANKL (Receptor Activator of Nuclear Factor-κ B Ligand) was used at 20 nM. Cells were cultured for four days with a renewal of the medium at day 2.

Human osteoclast precursors were purified from blood samples from healthy donors (obtained from the EFS, Etablissement Français du Sang, Marseille, France). Human CD11b$^+$ cells were purified using a CD11b MicroBeads kit (catalogue # 130-049-601) from Miltenyi Biotec (Paris, France) according to the manufacturer's instructions. For osteoclastic differentiation experiments, CD11b$^+$ cells were seeded at 30,000 cells/cm^2 in α-MEM containing 10% Hyclone serum, and cultured in the presence of 33 ng/mL hM-CSF and 66 ng/mL hRANKL as previously described [25].

2.3. Human cytokines and mouse effectors production (GST control protein, RANKL)

Human recombinant cytokines were purchased from PeproTech (Recombinant Human M-CSF, #300-25; Recombinant Human soluble RANK Ligand, #310-01). Mouse effectors were produced as fusion proteins with GST. GST-Rankl was produced as previously described [26]. For all the experiments using cells of murine origin, a GST protein, produced and purified using the same protocol, was used as a control.

2.4. Real-time PCR experiments

Total RNA samples were prepared using NucleoSpin RNA II kit (Macherey Nagel, Hoerdt, France), and reverse transcription (Superscript II/Rnase H$^-$/Reverse transcriptase, Invitrogen) was performed with 1 μg of RNA and random primers. A 10-fold dilution of cDNAs was used in amplification reactions. PCR experiments reported in Table 1 were performed using an ABI PRISM 7000 system (Applied Biosystems, Life Technologies SAS, Villebon-sur-Yvette, France), and qPCR Mastermix Plus was purchased from Eurogentec (Eurogentec France SASU, Angers, France). Reactions were performed in a 20 μL final volume using 5 μL of diluted cDNAs. Amplification conditions were as follows: 50 °C, 2 min; 95 °C, 10 min; (95 °C, 15 s; 60 °C, 1 min) cycled 40 times. The 36B4 housekeeping gene (Acidic Ribosomal Phosphoprotein P0) was used for normalization of the results. Real-time PCR reactions were performed using mouse and human gene-specific primers listed in Tables 1 and 2.

2.5. Immunolabeling

Cells were grown on glass coverslips in 24-well plates. After fixation and blocking with PBS containing 10% normal goat serum

Table 1
Mouse gene-specific primers used for real time RT-PCR analysis.

Mouse gene	Primer sequence	GI
36B4	Forward 5′-tccaggctttgggcatca-3′ Reverse 5′-cgctgggaacactcgatagg-3′	118131200
Nfatc1	Forward 5′-tgaggctggtcttccgagtt-3′ Reverse 5′-cgctgggaacactcgatagg-3′	118131200
Traf6	Forward 5′-aactgtgctgtgtccatggc-3′ Reverse 5′-cagtctcatgtgcaactggg-3′	38348245
Sqstm1 (p62)	Forward 5′-atgtggaacatggagggaaga-3′ Reverse 5′-ggagttcacctgtagatgggt-3′	118130186
Cyld	Forward 5′-caacatggatgccaggttgc-3′ Reverse 5′-gcctgaactcattgtgacagta-3′	28972434
c-Fos	Forward 5′-gggacagcctttcctactaccat-3′ Reverse 5′-gatctgcgcaaaagtcctgtg-3′	31560587

Table 2
Human gene-specific primers used for real time RT-PCR analysis.

Human gene	primer sequence	GI
36B4	Forward 5′-tgcatcagtaccccattctatcat-3′ Reverse 5′-aggcagatggatcagccaaga-3′	49087144
NFATC1	Forward 5′-gcatcacagggaagaccgtgtc-3′ Reverse 5′-gaagttcaatgtcggagtttctgag-3′	27502392
JDP2	Forward 5′-cttcttcttgttccggcatc-3′ Reverse 5′-cttcctggaggtgaaactgg-3′	205277415
JUND	Forward 5′-gtctacgcgaacctgagcagcta-3′ Reverse 5′-ctcgtccttgagcgcagccaggc-3′	169234622
FRA2	Forward 5′-tagatatgcctggctcaggcag-3′ Reverse 5′-ggttggacatggaggtgatcac-3′	44680151
C-FOS	Forward 5′- tgcctctcctcaatgaccctga-3′ Reverse 5′-ataggtccatgtctggcacgga-3′	6552332
ATP6V0A3	Forward 5′-gaagaggaacatgagcagcc-3′ Reverse 5′-ccgctaccaggaggtcaac-3′	19924144
ACP5	Forward 5′-gaccaccttggcaatgtctctg-3′ Reverse 5′-tggctgaggaagtcatctgagttg-3′	161377452
MMP9	Forward 5′-gtgctgggctgctgctttgctg-3′ Reverse 5′-gtcgccctcaaaggtttggaat-3′	74272286
CTR	Forward 5′-tggtgccaaccactatccatgc-3′ Reverse 5′-cacaagtgccgccatgacag-3′	46361988
ITGB3	Forward 5′-cattactctgcctccactacca-3′ Reverse 5′-aacggattttcccataagca-3′	47078291
BIM	Forward 5′-atccccgcttttcatcttta-3′ Reverse 5′-aggacttggggtttgtgttg-3′	116734657
BCLXL	Forward 5′-atggcagcagtaaagcaagc-3′ Reverse 5′-cggaagagttcattcactacctgt-3′	20336334
BCL2	Forward 5′-atgtgtgtggagagcgtcaacc-3′ Reverse 5′-tgagcagagtcttcagagacagcc-3′	72198188
BAX	Forward 5′-gctgttgggctggatccaag-3′ Reverse 5′-tcagcccatcttcttccaga-3′	163659848
BAD	Forward 5′-cgagtgagcaggaagactcca-3′ Reverse 5′-aggagtccacaaactcgtcact-3′	197116381

for 20 min at room temperature, cells were incubated with a 1/50 dilution of an anti-Nfatc1 antibody (Cat. # sc-7294, Santa Cruz Biotechnology, Heidelberg, Germany) or with a 1/50 dilution of an anti-NFkB antibody (Cat. # 4764S, Cell Signaling Technology, Danvers, MA 01923) in PBS containing 1.5% normal goat serum (Rockland, Gilbertsville, USA), for 60 min at room temperature. After washes in PBS, cells were subsequently incubated with a 1/500 dilution of a secondary antibody coupled to FITC (Cat. # sc-2010, Santa Cruz Biotechnology, Heidelberg, Germany), in PBS containing 3% normal goat serum, for 45 min at room temperature in the dark. Cells were counterstained with DAPI (Fig. 3A) or Topo-3 (Fig. 3B) for nuclear staining. Immunofluorescence was visualized using a confocal laser scanning microscope (LSM5, Zeiss).

2.6. Western-blot

RAW 264.7-cells were lysed in lysis buffer containing 0.2% Nonidet 40, 50 mM Tris, pH 7.5, 0.1 mM EDTA, pH 8.0, 0.1 mM EGTA, pH 8.0, 1 mM DTT, including a protease inhibitor cocktail (“Complete Mini”, Roche Diagnostics, Meylan, France) and phosphatase inhibitors (50 mM NaF and 1 mM Na_3VO_4). Following a centrifugation step at 15,000 × *g* for 15 min, protein concentration in the supernatant was determined using a BCA Protein Assay Kit from Pierce (Perbio Science). Proteins were separated by SDS-PAGE on 10% gels, and transferred to polyvinylidene difluoride (PVDF) membranes. Membranes were blocked with 5% BSA in Tris-buffered saline (TBS) containing Tween-20 (TTBS) at room temperature for 1 h 30 and then incubated for 2 h with primary antibodies: mouse anti-phospho-IκB (Cat. # 9246), mouse anti-IκB (Cat. # 4814), mouse anti-phospho-Akt (Cat. # 4051), mouse anti-Akt (Cat. # 2967), mouse anti-phospho-CREB (Cat. # 9196), mouse anti-β-Actin (Cat. # 3700) (all primary antibodies were from Cell Signaling Technology, Danvers, MA 01923). Horseradish peroxidase-conjugated anti-mouse antibody (Cat. # sc-2005, Santa Cruz Biotechnology, Heidelberg, Germany) was used as a secondary antibody (45 min incubation). The antigen–antibody complexes were visualized using ECL Plus Kit (Amersham Biosciences, Piscataway, USA).

2.7. Measurement of intracellular Ca^{2+} oscillations

$CD11^+$ cells suspended at 1.5×10^6 cells/mL in HBSS were preincubated with 100 μM Ga for 1 h at 37 °C. Cells were loaded during 30 min with cell-permeable calcium indicators, in HBSS medium containing 2.6 μM Fluo-3 AM (Cat. # F-1242) and 5.5 μM Fura-Red AM (Cat. # F-3021) (calcium indicators were from Invitrogen Corporation, Paisley, UK). Cells were next washed once and resuspended in HBSS medium (1.5×10^6 cells/mL). Where noted, reagents including ionomycin, EGTA, gallium, and gadolinium were added to the medium after an equilibration period of 1 min. Using specific filters, the Fluo-3/Fura-Red emission ratio of fluorescence was analyzed by flow cytometry (FACS Aria cytometer, BD Biosciences, Le Pont de Claix, France).

2.8. Statistical analysis

The data shown is representative of at least three independent experiments. Results are expressed as mean ± standard deviation of three determinations. The statistical differences between two independent groups were evaluated using the Mann & Whitney test (bi-directional analysis). Comparative analysis of more than two independent groups was performed using the Kruskall–Wallis test (bi-directional analysis). The differences measured were considered to be statistically significant for $p < 0.05$.

3. Results

3.1. Effects of Ga on differentiation and survival of human osteoclasts

Human $CD11b^+$ cells isolated from peripheral blood were cultured in differentiating medium for 2 or 7 days, before a 12-h incubation in the presence of 100 μM Ga, the pharmacological dose which was demonstrated to be optimal in our previous study [14]. As depicted in Fig. 1A, 100 μM Ga significantly down-regulated the expression of specific osteoclastic differentiation early marker genes including *NFATC1*, *FRA2*, *JDP2* and *JUND*. Conversely, when cells were incubated in the presence of 100 μM Ga after seven days of differentiation, Ga did not modify the expression of specific osteoclastic differentiation late marker genes such as *ACP5*, *ATP6VOA3*, *MMP9*, *CTR* and *ITGB3* (Fig. 1A).

On the whole, a 12-h Ga treatment inhibited the induction of early differentiation marker gene expression, while the same treatment performed subsequently did not modify the expression of late differentiation marker genes.

As RANKL and M-CSF are also largely involved in osteoclastic survival, we wanted to determine whether Ga may have an effect on apoptosis induction both in precursor and mature osteoclasts. Thus, we explored Ga impact on the expression of pro- and anti-apoptotic genes. Human $CD11b^+$ cells were differentiated in the presence of hM-CSF and hRANKL. After 2 or 7 days, cells were treated for 12 h with 100 μM Ga (Fig. 1B), and the expression of pro- and anti-apoptotic genes was quantified by RT-PCR. As shown in Fig. 1B, Ga treatment did not affect the expression of the most prominent pro- and antiapoptotic factors, as measured in both osteoclastic precursor cells and in mature osteoclasts.

3.2. Ga effect on Nfatc1 expression

Given that Ga disturbed expression of early marker genes (Fig. 1A), we next focused on this early phase of osteoclastic differentiation, and more particularly on the initial induction of

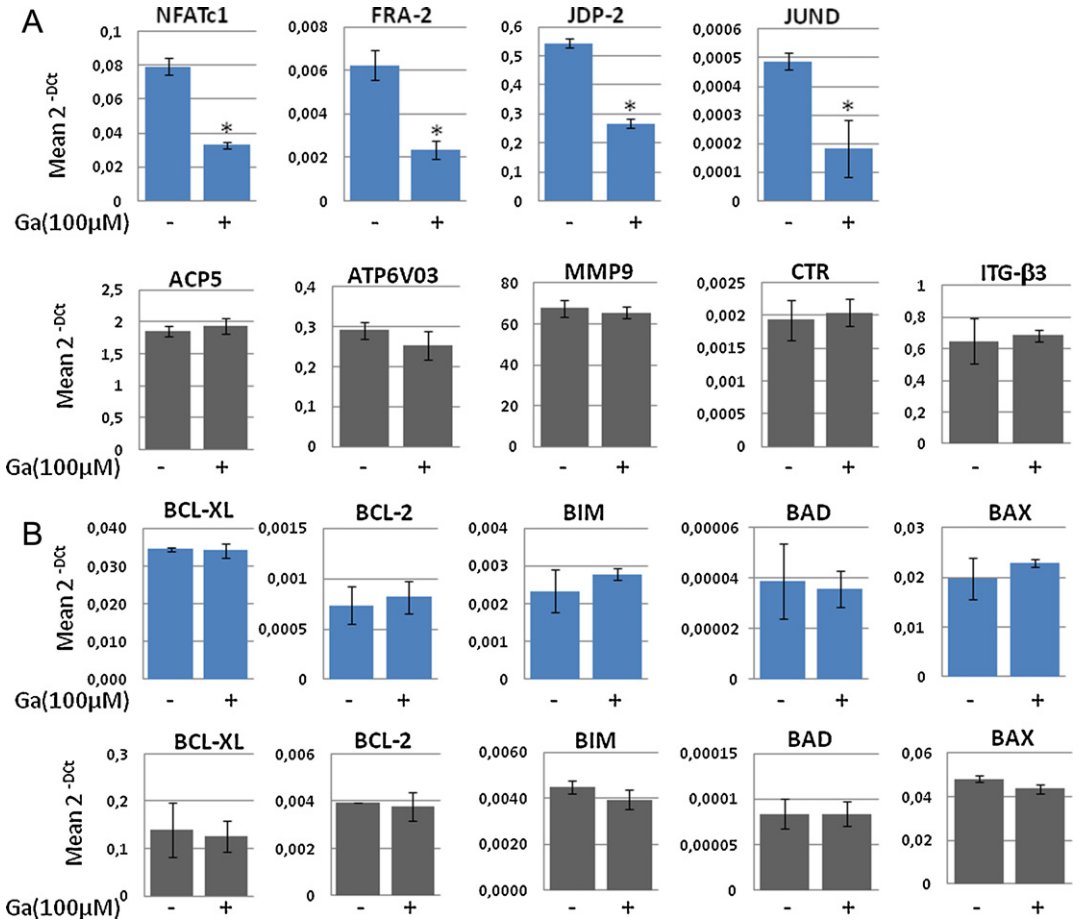

Fig. 1. Ga effect on differentiation (A) and apoptosis (B) of osteoclasts. Human CD11b$^+$ cells were cultured in the presence of 33 ng/mL hM-CSF and 66 ng/mL hRANKL. After two days (blue) or seven days (gray), cells were treated for 12 h with 100 μM Ga (+) or its vehicle (−). Quantitative real-time PCR analysis was performed using *36B4* as housekeeping gene. $^*p < 0.05$, statistically significant compared to untreated cells (Mann & Whitney test, bidirectional analysis). (A) Real time PCR analysis of the main osteoclastic differentiation marker genes. (B) Real time PCR analysis of the main cellular survival and apoptosis marker genes. (For interpretation of the references to color in the text, the reader is referred to the web version of the article.)

Nfact1 gene expression, and the auto-amplification step that leads to Nfatc1 protein level upregulation.

We had previously demonstrated that Ga reduced, in a dose-dependent manner, the initial induction of *Nfatc1* gene in RAW 264.7 cells incubated in the presence of Rankl for 12 and 24 h [14]. To investigate Ga impact on the auto-amplification stage, which occurs subsequent to the initial induction, we measured *Nfatc1* gene expression after a 48 h incubation period of cells with both Rankl and Ga. As shown in Fig. 2A, Ga induced a downregulation of *Nfatc1* gene expression, and this inhibition reached 40% when 100 μM Ga was used.

To correlate these effects of Ga at the transcript level with Nfatc1 protein content, we performed immunolabeling of RAW 264.7 cells treated with RanklL/Ga for 48 h (Fig. 2B). In the absence of Rankl, we detected a weak labeling of cells (Fig. 2B, b), while Rankl treatment induced a strong expression of Nfatc1 protein expression (Fig. 2B, c and d). Lastly we observed that a 100 μM Ga treatment prevented Rankl-induced Nfatc1 protein expression (Fig. 2B, e and f).

In summary, we found that in addition to the initial induction of Nfatc1 (12–24 h), Ga treatment impacted latter amplification step (48 h), both at the transcript and protein levels.

3.3. Ga effect on initial induction of Nfatc1

As NFκB activation plays a critical role in initiating a robust induction of Nfatc1, we next wanted to decipher the effect of Ga on the NFκB signaling pathway.

The phosphorylation of IκB is a marker for ubiquitination and subsequent proteasome-mediated degradation. The degradation of inhibitory κB (IκB) unmasks the nuclear localization signal motif of NFκB, thus allowing its nuclear translocation and participation in the initial induction of *Nfatc1* gene expression. As shown in Fig. 3A, Rankl induced IκB phosphorylation within 15 min. Concomitantly, IκB protein was degraded, as shown at 30 min, before resynthesis between 45 and 60 min. Ga did not block IκB phosphorylation, but rather weakly stimulated it at 45 min. In contrast, we observed that 100 μM Ga partially inhibited Rankl-induced IκB degradation detected at 30 and 45 min.

Overall, while Ga treatment did not reduce IκB phosphorylation within differentiating osteoclast progenitor cells, Ga partially and transitorily blocked Rankl-induced IκB degradation. To deepen Ga effect on NFκB signaling pathway, we determined whether this blockage had repercussions on nuclear NFκB translocation by performing immunostaining of NFκB protein. As shown in Fig. 3B(a), NFκB, which is preferentially located in the cytoplasm following a 15 min Rankl treatment, is progressively translocated within the nucleus as observed after a longer incubation period with Rankl. In contrast, a 100 μM Ga treatment blocked NFκB nuclear translocation, at least up to 45 min following Rankl addition (Fig. 3B, b).

Upstream signaling of NFκB by Rankl involves the recruitment of Traf6 following the binding of Rankl to its receptor Rank. In addition, NFκB nuclear translocation is mediated by the interaction of Traf6 with p62 and IKK [27]. Moreover, p62 interacts with deubiquitinating enzyme Cyld to negatively regulate Rank signaling [28]. Thus, we next wanted to evaluate Ga impact on

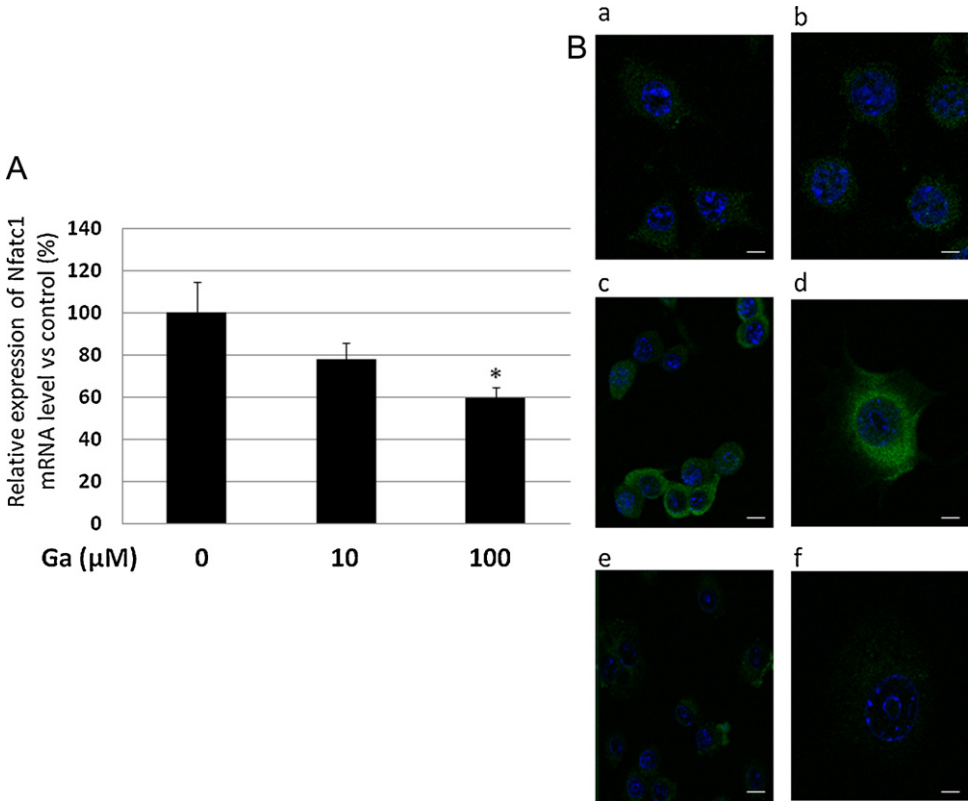

Fig. 2. Ga effect on the expression of *Nfatc1* gene and Nfatc1 protein. (A) Real-time PCR analysis of *Nfatc1* gene expression. RAW 264.7 cells were differentiated for 48 h with 20 nM Rankl, in the presence of 10 μM or 100 μM Ga. Results are expressed as a percentage of *Nfatc1* gene expression level in control condition. $^{*}p < 0.05$, statistically significant compared to untreated cells (Kruskall–Wallis test, bidirectional analysis). (B) Immunostaining analysis of Nfatc1 protein expression. (a) Control immunostaining without primary antibody; (b) control differentiation without Rankl treatment; (c–f) RAW 264.7 cells were cultured for 48 h with 20 nM Rankl, in absence (c, d) or in presence (e, f) of 100 μM Ga. (bar = 10 μm).

Traf6, p62 and Cyld. As depicted on Fig. 4, we observed that 100 μM Ga significantly increased *Traf6*, *p62* and *Cyld* gene expression when compared to the quantification upon cells treatment with Rankl alone.

3.4. Ga effect on Nfatc1 auto-amplification

Nfatc1 positively regulates its own gene expression through an auto-amplification mechanism involving its recruitment to its own promoter as an AP-1 complex containing c-Fos [19,20,23]. Using RAW 264.7 cells, we observed that a 100 μM Ga treatment reduced Rankl-induced *c-Fos* gene expression by 53% in comparison to control condition (Fig. 5).

3.5. Ga effect on Rankl-induced Akt and Creb phosphorylation

Akt signaling is one of the pathways that interact with NFκB and *c-Fos* in response to Rankl [29,30]. Rankl stimulation triggers

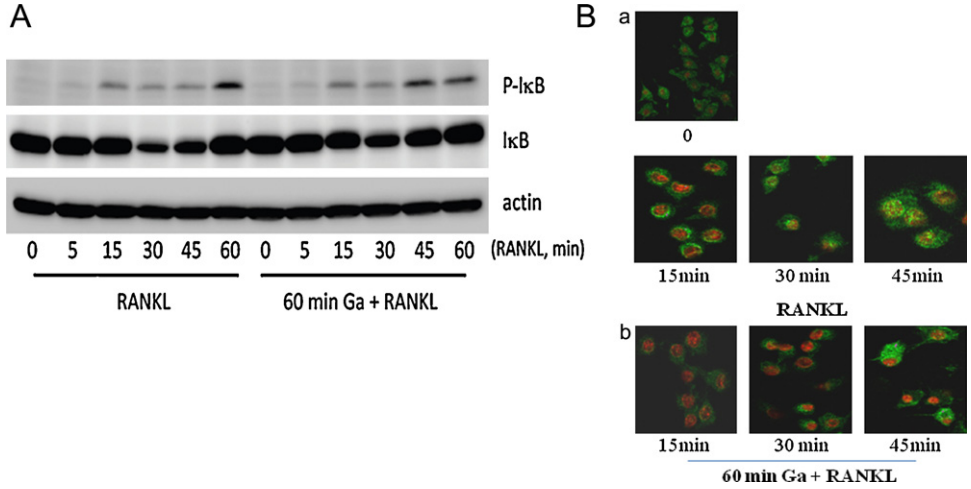

Fig. 3. Ga effect on Rankl-induced NFκB signaling pathway. (A) Ga effect on Rankl-induced IκB phosphorylation. RAW 264.7 cells were cultured for 16 h in serum-depleted medium containing 0.2% BSA, pretreated with 100 μM Ga (+) or its vehicle (−) for 1 h, and stimulated with 20 nM Rankl for the indicated time. Western-blot analysis of IκB phosphorylation. Cell extracts were analyzed using antibodies directed against the total form or the phosphorylated form of IκB (p-IκB). β-actin detection was used as a loading control. (B) Ga effect on Rankl-induced nuclear NFκB translocation. RAW 264.7 cells were cultured as described in (A). Next, cells were pretreated with 100 μM Ga (b) or its vehicle (a) for 1 h, and stimulated with 20 nM Rankl for the indicated time. Immunostaining analysis of NFκB protein expression was performed. (bar = 10 μm).

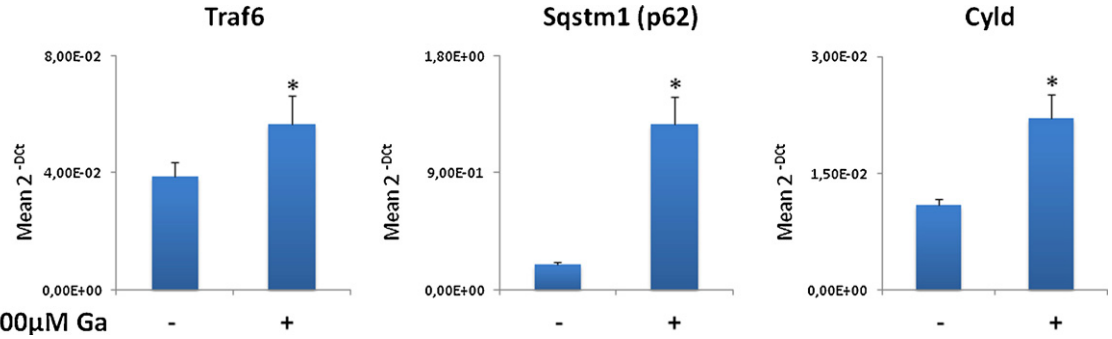

Fig. 4. Ga effect on Rankl-induced *Traf6, p62* and *Cyld* gene expression in mouse cells. Real-time PCR analysis of *Traf6, p62* and *Cyld* gene expression. RAW 264.7 cells were differentiated for 48 h with 20 nM Rankl, in the presence or in the absence of 100 μM Ga. Quantitative real-time PCR analysis was performed using *36B4* as housekeeping gene. $^{*}p < 0.05$, statistically significant compared to untreated cells (Mann & Whitney test, bi-directional analysis).

Akt phosphorylation, and p-Akt regulates the activity of IκB kinase (IKK), which phosphorylates IκB [31]. Phospho-Akt is also involved in the phosphorylation of the transcription factor Creb (cyclic AMP-responsive element-binding), and Creb-mediated induction of *c-Fos* is implied in the transcriptional control of *Nfatc1* during osteoclastogenesis [32]. Thus, we investigated Ga effect on Rankl-induced Akt- and Creb phosphorylation.

Using RAW 264.7 cells, and as shown in Fig. 6A, Rankl treatment induced the phosphorylation of both Akt and Creb. In addition, Ga pretreatment did not modify Rankl-induced phosphorylation of both Akt and Creb.

3.6. Ga effect on calcium signaling pathway

Ga has been shown to substitute calcium in biological apatite [9]. Considering the essential role of calcium signaling during osteoclastic differentiation, as well as the chemical similarity between Ga and calcium, we examined the effects of Ga on calcium-induced intracellular signaling and on calcium entry within osteoclast precursor cells.

Rankl activates calcium signaling, which triggers the CaMK-Creb pathway. As shown in Fig. 6A, Rankl stimulated Creb protein phosphorylation, and in these experimental conditions, a treatment with 100 μM of Ga did not exert any inhibitory effect. In addition to the release of stores coming from the endoplasmic reticulum, intracellular calcium oscillations may also result from the entry of extracellular calcium through specific calcium channels present at the cell surface. Thus, we studied Creb phosphorylation in response to extracellular calcium, in the presence or in the absence of gallium. As shown in Fig. 6B, a 10 min treatment of RAW 264.7 cells with 10 mM Ca^{2+} induced a strong upregulation of Creb phosphorylation. In contrast, a 1 h cells pretreatment with 100 μM Ga completely reversed the calcium-induced Creb phosphorylation.

Lastly, we wanted to determine whether Ga could interfere with extracellular calcium uptake through a specific calcium channel, i.e. TRPV-5A (Transient Receptor Potential cation channel subfamily V member 5A). TRPV-5A is a calcium channel highly expressed in human osteoclasts [33], and which is largely involved in intracellular calcium oscillations. Using gadolinium (Gd) as a specific agonist of this channel, as well as human $CD11b^{+}$ cells, we examined whether Ga may block calcium entry through this channel. As shown in Fig. 7, the addition of 50 μM Gd induced a significant increase in intracellular calcium in $CD11b^{+}$ cells. In contrast, when cells were simultaneously treated with 50 μM Gd and 100 μM Ga, Gd did not trigger anymore intracellular calcium increase.

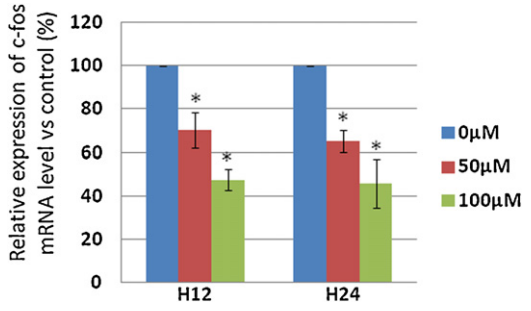

Fig. 5. Ga effect on Rankl-induced *c-Fos* gene expression in mouse cells. Real-time PCR analysis of *c-Fos* gene expression in mouse cells. RAW 264.7 cells were cultured with 20 nM Rankl, and 50 μM or 100 μM of Ga for 12 and 24 h. Results are expressed as a percentage of *c-Fos* gene expression level in control condition. $^{*}p < 0.05$, statistically significant compared to untreated cells (Kruskall–Wallis test, bidirectional analysis).

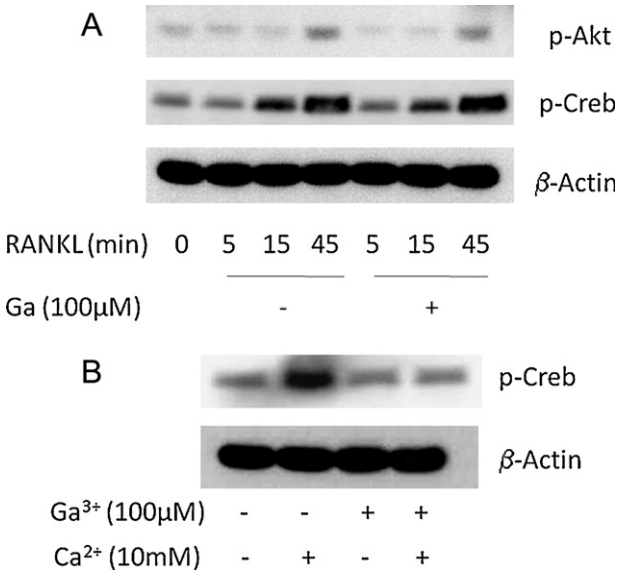

Fig. 6. Ga effect on Akt and CREB phosphorylation in mouse cells. (A) Western-blot analysis of Rankl-stimulated Akt and Creb phosphorylation. RAW 264.7 cells were cultured for 16 h in serum-depleted media containing 0.2% BSA, pretreated with 100 μM Ga (+) or its vehicle (−) for 1 h, and stimulated with 20 nM Rankl for the indicated time. Cell extracts were analyzed using antibodies directed against the phosphorylated forms of Akt (p-Akt) or Creb (p-Creb). β-actin detection was used as a loading control. (B) Western-blot analysis of Ca^{2+}-stimulated Creb phosphorylation. RAW 264.7 cells were starved for 5 h in DMEM containing 0.2% BSA, preincubated with 100 μM Ga (+) or its vehicle (−) for 1 h, and treated (+) or not (−) with 10 mM Ca^{2+} for 10 min. Cell extracts were analyzed using antibodies directed against the phosphorylated form of creb (p-creb). β-actin detection was used as a loading control.

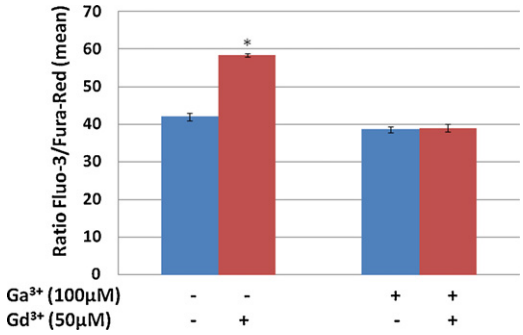

Fig. 7. Ga effect on $Ca^{2\pm}$ uptake in human cells. Flow cytometry analysis of gadolinium-stimulated calcium uptake. Human $CD11b^+$ cells were loaded with Fluo-3 and Fura-Red for 30 min. Cells were treated with (+) or without (−) 100 μM Ga and 50 μM Gd. After 5 min, Ca^{2+} uptake was monitored for 1 min. Results are expressed as the mean of Fluo-3/Fura-Red emission ratio (n = 7).

On the whole, using osteoclast precursors pretreated with Ga, we observed an inhibition of calcium-induced Creb phosphorylation, as well as a blocking of gadolinium-induced calcium entry through the TRPV-5A calcium channel.

4. Discussion

In our previous studies, we demonstrated that Ga inhibited the process of osteoclastic differentiation in a dose-dependent manner, which results in blocking osteoclast resorptive activity [14]. To obtain pertinent results about a potential distinct sensitivity to Ga of precursor and mature cells respectively, we investigated this issue using human $CD11b^+$ cells isolated from peripheral blood as a source of osteoclast progenitors [25]. We observed that Ga specifically affected the expression of marker genes within differentiating osteoclastic precursors rather than in mature osteoclasts. Furthermore, we observed that Ga did not disturb the expression of pro and antiapoptotic markers both in precursor and mature osteoclasts. These data confirm our preliminary experiment performed on mature osteoclasts obtained upon RAW 264.7 cells differentiation, a cell line that is considered more resistant than human primary cells. Results obtained from a human model of osteoclast-like cells strengthen the relevance of our basic data. For practical reasons, we continued using the murine RAW 264.7 cells.

We had previously reported that Ga reduced the expression of *Nfatc1* gene in a dose-dependent manner at the early stages (12–24 h) of osteoclastic differentiation in the murine RAW 264.7 cell line [14]. Using the same model, we show here that this inhibitory effect of Ga on *Nfatc1* gene expression persists for 48 h in Rankl-treated cells (Fig. 2A), and that this transcriptional effect impacts Nfatc1 protein content of the cells (Fig. 2B). From these results, we conclude that Ga inhibits both the initial and auto-amplification steps of Nfatc1 induction (Fig. 8).

Focusing on NFκB activation, we have documented Ga impact on the initial induction of Nfatc1. NFκB forms a complex with its inhibitory element (IκB) that prevents its translocation into the nucleus. Phosphorylation of IκB induces its own degradation resulting in activation of NFκB. As shown in Fig. 3A, Ga partially protect IκB from degradation without inhibiting its phosphorylation. This result, suggesting that Ga interacts with IκB degradation, is in accordance with a study from Chen et al. [34], which describes an inhibition of the proteasome activity by gallium(III) complexes. Furthermore, Ang et al. reported in 2009 [35] that proteasome inhibitors modulate NF-κB activation and osteoclast formation. We hypothesize that by blocking proteasome-mediated IκB degradation, p-IκB protein accumulates in the cytoplasm (Fig. 3).

Further supports to this hypothesis come from our data on Traf6 and p62. Traf6 is known to interact with p62 and IKK, thereby mediating IκB degradation [36]. We demonstrate that 100 μM Ga increases *Traf6* and *p62* gene expression (Fig. 4), and this is interesting considering that the accumulation of p62 appears to impact the ubiquitine/proteasome system by delaying the delivery of ubiquitinated proteins to the proteasome [27]. Thus, signaling

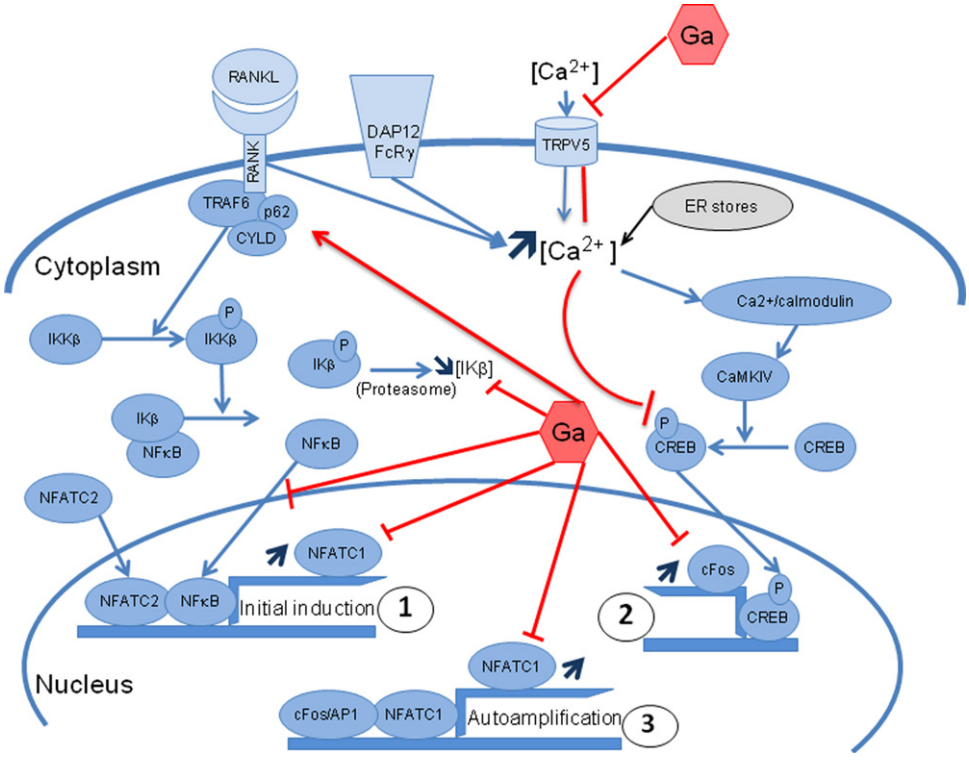

Fig. 8. Molecular targets of Ga action on osteoclast precursor cells differentiation.

repression observed upon p62 overexpression in NFkB reporter assays might be explained by an impaired clearance of IκB via the ubiquitine proteasome system [36]. Ga-induced *Cyld* overexpression further documents the molecular mechanisms of Ga action on NFkB signaling pathway (Fig. 4). Cyld is a deubiquitinating enzyme which is considered as a crucial negative regulator of osteoclastogenesis [28]. Indeed, Cyld appears to be recruited through a direct interaction with the p62, and this negatively regulates NFkB pathway by removing the ubiquitin modification from TRAF6 [36]. As a whole, these data contribute to explain how NFkB signaling pathway, and more specifically IκB degradation, is impaired upon Ga treatment.

To determine whether IκB degradation inhibition had an impact on nuclear NFκB translocation, we studied cellular localization of NFκB following Ga treatment by performing immunostaining analysis (Fig. 3B). In the absence of Ga treatment, NFκB translocates within the nuclear compartment following a 45 min Rankl treatment. By contrast, the treatment with 100 μM Ga, maintained preferentially NFκB within the cytoplasm. Overall, the inhibition of IκB degradation observed with 100 μM Ga treatment was accompanied by a blockage of Rankl-induced NFκB nuclear translocation, this leading to the disruption of Nfatc1 initial induction (Fig. 8).

We also observe that Ga down-regulates *c-Fos* gene expression within differentiating osteoclast progenitors. Thus, we conclude that Ga also impacts the auto-amplification of Nfatc1, since c-Fos is known to be critical for this stage of osteoclastic differentiation [23].

To further investigate the molecular mechanisms of Ga action, we were interested in finding intracellular targets that could interact with both NFκB and c-Fos. We focused on Akt, a downstream target of PI3K, which is also activated by Rankl [29,30].

In the canonical pathway, Akt activates the IKK complex that phosphorylates and degrades IκB [31], and Sugatani et al. have shown that Akt regulates NFκB activity through an Akt phosphorylation site present within the IKK complex [37]. Our data clearly indicate a lack of Ga effect on Akt activation, this indicating that Ga effect on IκB phosphorylation we observe at 45 min (Fig. 3) is not mediated through Akt. Akt phosphorylates also the transcription factor Creb, which regulates *c-Fos* expression [32]. However, according to the literature, Rankl-induced *c-Fos* expression is only partially understood. In our study, pretreatment with 100 μM Ga for 1 h did not alter the activation of either Akt or Creb in response to Rankl. From these data, it is unlikely that Ga directly modulates *c-Fos* expression via Creb.

NFκB activation occurs through two distinct mechanisms. The most important mechanism is based on IκB phosphorylation that governs the proteasome-mediated IκB degradation. This mechanism includes both classical (canonical) and alternative (non-canonical) NFκB signaling pathways. In contrast to this phosphorylation process, another NFκB activation pathway through the polymerization-mediated depletion of free IκB has been recently described [38]. This pathway is mediated by transglutaminase 2 (TGase 2)/μcalpain. Briefly, TGase 2 is a crosslinking enzyme involved in cellular processes such as cell migration, adhesion, and differentiation. TGase 2 induces polymerization of IκB which becomes a substrate for μcalpain, a non-lysosomal thiolprotease [39]. This proteolytic pathway is independent of the ubiquitin-proteasome degradation system. It will be interesting to investigate the effects of Ga on this pathway, especially considering that the activity of these enzymes (TGase 2 and μcalpain) depends on calcium ions.

Although many unknowns remain concerning how Ca^{2+} signaling triggers Nfatc1 activation, Ca^{2+} is critical for osteoclastic proliferation, differentiation and survival. For example, the Ca^{2+}-CaMK-Creb pathway is not only important for the initial induction of *c-Fos* but it also regulates the expression of osteoclast-specific genes in cooperation with Nfatc1 [23]. In addition, it is now well-established that osteoclasts can sense environmental level of Ca^{2+} through the Ca-sensing receptor (CaR) leading to intracellular signaling which notably stimulates Creb phosphorylation and therefore differentiation of osteoclasts [40]. Using mouse RAW 264.7 cells stimulated with an elevated extracellular Ca^{2+} concentration, we observe that Ga completely inhibits calcium-induced Creb phosphorylation. This result suggests an interaction between Ga and calcium signaling.

Given the chemical similarity of Ga and calcium, we hypothesized that Ga may interact with Ca^{2+}-signal by blocking Ca^{2+} entry. Extracellular Ca^{2+} entry is of particular importance for human osteoclasts since it is responsible for a significant increase in intracellular Ca^{2+} in response to RANKL. Indeed, in a human osteoclast model, Chamoux et al. showed that none of the traditional calcium-channels was involved in the RANKL-induced calcium spike [33]. They described that RANKL treatment opens a specific calcium-channel, namely TRPV-5, which belongs to the TRP channel family. This phenomenon allows extracellular Ca^{2+} entry, and thus intracellular oscillations of Ca^{2+} concentration independently from the signaling pathway involving PLCγ and intracellular calcium stores. In an effort to determine whether Ga may block this critical Ca-channel, we used gadolinium as a specific agonist of TRPV-5 in primary human osteoclast precursors isolated from peripheral blood, and we report that Ga completely abolishes intracellular Ca^{2+} oscillations induced by gadolinium. This result strongly suggests that Ga could also act by blocking a specific Ca-channel in the plasma membrane of osteoclasts, thus disturbing intracellular Ca^{2+} oscillations (Fig. 8).

5. Conclusion

In summary, we identify for the first time Traf6, p62, Cyld, IκB, NFκB, c-Fos, as well as calcium-induced Creb phosphorylation, as molecular targets of Ga during osteoclast differentiation, this tremendously impacting the expression of the master transcription factor Nfatc1. In addition, our results strongly suggest that the TRPV-5 calcium channel, which is located within the plasma membrane, is a target of Ga action on human osteoclast progenitor cells.

Acknowledgements

The study was supported by grants from Fondation de l'Avenir (ET9-524) and Graftys SA.

References

[1] Lecoq de Boisbaudran PE. Annales de Chimie Série 5 1877;10:100–41.
[2] Bernstein LR. Mechanisms of therapeutic activity for gallium. Pharmacol Rev 1998;50:665–82.
[3] Collery P, Keppler B, Madoulet C, Desoize B. Gallium in cancer treatment. Crit Rev Oncol Hematol 2002;42:283–96.
[4] Krakoff IH, Newman RA, Goldberg RS. Clinical toxicologic and pharmacologic studies of gallium nitrate. Cancer 1979;44:1722–7.
[5] Warrell Jr RP, Bockman RS, Coonley CJ, Isaacs M, Staszewski H. Gallium nitrate inhibits calcium resorption from bone and is effective treatment for cancer-related hypercalcemia. J Clin Invest 1984;73:1487–90.
[6] Warrell Jr RP, Israel R, Frisone M, Snyder T, Gaynor JJ, Bockman RS. Gallium nitrate for acute treatment of cancer-related hypercalcemia. A randomized, double-blind comparison to calcitonin. Ann Intern Med 1988;108:669–74.
[7] Warrell Jr RP, Bosco B, Weinerman S, Levine B, Lane J, Bockman RS. Gallium nitrate for advanced Paget disease of bone: effectiveness and dose-response analysis. Ann Intern Med 1990;113:847–51.
[8] Bockman R. The effects of gallium nitrate on bone resorption. Semin Oncol 2003;30:5–12.
[9] Korbas M, Rokita E, Meyer-Klaucke W, Ryczek J. Bone tissue incorporates in vitro gallium with a local structure similar to gallium-doped brushite. J Biol Inorg Chem 2004;9:67–76.

[10] Bockman RS, Boskey AL, Blumenthal NC, Alcock NW, Warrell Jr RP. Gallium increases bone calcium and crystallite perfection of hydroxyapatite. Calcif Tissue Int 1986;39:376–81.
[11] Bockman RS, Repo MA, Warrell Jr RP, Pounds JG, Schidlovsky G, Gordon BM, et al. Distribution of trace levels of therapeutic gallium in bone as mapped by synchrotron x-ray microscopy. Proc Natl Acad Sci USA 1990;87:4149–53.
[12] Hall TJ, Chambers TJ. Gallium inhibits bone resorption by a direct effect on osteoclasts. Bone Miner 1990;8:211–6.
[13] Blair HC, Teitelbaum SL, Tan HL, Schlesinger PH. Reversible inhibition of osteoclastic activity by bone-bound gallium (III). J Cell Biochem 1992;48: 401–10.
[14] Verron E, Masson M, Khoshniat S, Duplomb L, Wittrant Y, Baud'huin M, et al. Gallium modulates osteoclastic bone resorption in vitro without affecting osteoblasts. Br J Pharmacol 2010;159:1681–92.
[15] Blair HC. How the osteoclast degrades bone. Bioessays 1998;20:837–46.
[16] Suda T, Takahashi N, Martin TJ. Modulation of osteoclast differentiation: update 1995. Endocr Rev 1995;4:266–70.
[17] Theill LE, Boyle WJ, Penninger JM. RANK-L and RANK: T cells, bone loss, and mammalian evolution. Annu Rev Immunol 2002;20:795–823.
[18] Lagasse E, Weissman IL. Enforced expression of Bcl-2 in monocytes rescues macrophages and partially reverses osteopetrosis in op/op mice. Cell 1997;89:1021–31.
[19] Asagiri M, Sato K, Usami T, Ochi S, Nishina H, Yoshida H, et al. Autoamplification of NFATc1 expression determines its essential role in bone homeostasis. J Exp Med 2005;202:1261–9.
[20] Asagiri M, Takayanagi H. The molecular understanding of osteoclast differentiation. Bone 2007;40:251–64.
[21] Takayanagi H. The role of NFAT in osteoclast formation. Ann N Y Acad Sci 2007;1116:227–37.
[22] Takayanagi H, Kim S, Koga T, Nishina H, Isshiki M, Yoshida H, et al. Induction and activation of the transcription factor NFATc1 (NFAT2) integrate RANKL signaling in terminal differentiation of osteoclasts. Dev Cell 2002;3: 889–901.
[23] Negishi-Koga T, Takayanagi H. Ca_2^+-NFATc1 signaling is an essential axis of osteoclast differentiation. Immunol Rev 2009;231:241–56.
[24] Takayanagi H. Mechanistic insight into osteoclast differentiation in osteoimmunology. J Mol Med 2005;83:170–9.
[25] Mouline CC, Quincey D, Laugier JP, Carle GF, Bouler JM, Rochet N, et al. Osteoclastic differentiation of mouse and human monocytes in a plasma clot/biphasic calcium phosphate microparticles composite. Eur Cell Mater 2010;20:379–92.
[26] Beranger GE, Momier D, Guigonis JM, Samson M, Carle GF, Scimeca JC. Differential binding of poly(ADP-Ribose) polymerase-1 and JunD/Fra2 accounts for RANKL-induced Tcirg1 gene expression during osteoclastogenesis. J Bone Miner Res 2007;22:975–83.
[27] Korolchuk VI, Mansilla A, Menzies FM, Rubinsztein DC. Autophagy inhibition compromises degradation of ubiquitin-proteasome pathway substrates. Mol Cell 2009;33:517–27.
[28] Jin W, Chang M, Paul EM, Babu G, Lee AJ, Reiley W, et al. Deubiquitinating enzyme CYLD negatively regulates RANK signaling and osteoclastogenesis in mice. J Clin Invest 2008;118:1858–66.
[29] Wong BR, Besser D, Kim N, Arron JR, Vologodskaia M, Hanafusa H, et al. TRANCE, a TNF family member, activates Akt/PKB through a signaling complex involving TRAF6 and c-Src. Mol Cell 1999;4:1041–9.
[30] Lee SE, Woo KM, Kim SY, Kim HM, Kwack K, Lee ZH, et al. The phosphatidylinositol 3-kinase, p38, and extracellular signal-regulated kinase pathways are involved in osteoclast differentiation. Bone 2002;30:71–7.
[31] Ozes ON, Mayo LD, Gustin JA, Pfeffer SR, Pfeffer LM, Donner DB. NF-kappaB activation by tumour necrosis factor requires the Akt serine-threonine kinase. Nature 1999;401:82–5.
[32] Sato K, Suematsu A, Nakashima T, Takemoto-Kimura S, Aoki K, Morishita Y, et al. Regulation of osteoclast differentiation and function by the CaMK-CREB pathway. Nat Med 2006;12:1410–6.
[33] Chamoux E, Bisson M, Payet MD, Roux S. TRPV-5 mediates a RANK ligand-induced increase in cytosolic Ca^{2+} in human osteoclasts and downregulates bone resorption. J Biol Chem 2010;285:25354–62.
[34] Chen D, Frezza M, Shakya R, Cui QC, Milacic V, Verani CN, et al. Inhibition of the proteasome activity by gallium(III) complexes contributes to their anti prostate tumor effects. Cancer Res 2007;67:9258–65.
[35] Ang ES, Zhang P, Steer JH, Tan JW, Yip K, Zheng MH, et al. Calcium/calmodulin-dependent kinase activity is required for efficient induction of osteoclast differentiation and bone resorption by receptor activator of nuclear factor kappa B ligand (RANKL). J Cell Physiol 2007;212:787–95.
[36] Goode A, Layfield R. Recent advances in understanding the molecular basis of Paget disease of bone. J Clin Pathol 2010;63:199–203.
[37] Sugatani T, Hruska KA. Akt1/Akt2 and mammalian target of rapamycin/Bim play critical roles in osteoclast differentiation and survival, respectively, whereas Akt is dispensable for cell survival in isolated osteoclast precursors. J Biol Chem 2005;280:3583–9.
[38] Kim DS, Han BG, Park KS, Lee BI, Kim SY, Bae CD. I-kappaBalpha depletion by transglutaminase 2 and mu-calpain occurs in parallel with the ubiquitin-proteasome pathway. Biochem Biophys Res Commun 2010;399:300–6.
[39] Lee FY, Kim DW, Karmin JA, Hong D, Chang SS, Fujisawa M, et al. mu-Calpain regulates receptor activator of NF-kappaB ligand (RANKL)-supported osteoclastogenesis via NF-kappaB activation in RAW 264.7 cells. J Biol Chem 2005;280:29929–33.
[40] Seuwen K, Boddeke HG, Migliaccio S, Perez M, Taranta A, Teti A. A novel calcium sensor stimulating inositol phosphate formation and $[Ca_2^+]_i$ signaling expressed by GCT23 osteoclast-like cells. Proc Assoc Am Physicians 1999;111: 70–81.